Applied Physics Letters

RESEARCH ARTICLE | FEBRUARY 05 2013

Nanoscale structure of protamine/DNA complexes for gene delivery

Simona Motta; Paola Brocca; Elena Del Favero; Valeria Rondelli; Laura Cantù; Augusto Amici; Daniela Pozzi; Giulio Caracciolo

Appl. Phys. Lett. 102, 053703 (2013)
https://doi.org/10.1063/1.4790588

Nanoscale structure of protamine/DNA complexes for gene delivery

Simona Motta,[1] Paola Brocca,[1,a)] Elena Del Favero,[1] Valeria Rondelli,[1] Laura Cantù,[1] Augusto Amici,[2] Daniela Pozzi,[3] and Giulio Caracciolo[3]
[1]*Dipartimento di Biotecnologie Mediche e Medicina Traslazionale, Università degli Studi di Milano, Via F.lli Cervi, 93, 20090 Segrate (MI), Italy*
[2]*Dipartimento di Bioscienze e Biotecnologie, Università di Camerino, Via Gentile III da Varano, 62032 Camerino (MC), Italy*
[3]*Dipartimento di Medicina Molecolare, Sapienza Università di Roma, Viale Regina Elena, 324, 00161 Rome, Italy*

(Received 7 November 2012; accepted 21 January 2013; published online 5 February 2013)

Understanding the internal packing of gene carriers is a key-factor to realize both gene protection during transport and de-complexation at the delivery site. Here, we investigate the structure of complexes formed by DNA fragments and protamine, applied in gene delivery. We found that complexes are charge- and size-tunable aggregates, depending on the protamine/DNA ratio, hundred nanometers in size. Their compactness and fractal structure depend on the length of the DNA fragments. Accordingly, on the local scale, the sites of protamine/DNA complexation assume different morphologies, seemingly displaying clumping ability for the DNA network only for shorter DNA fragments. © *2013 American Institute of Physics*. [http://dx.doi.org/10.1063/1.4790588]

The delivery of genetic material into cells is indispensable for investigating gene function and conducting gene therapy.[1–4] Of primary importance is the design of effective and safe gene delivery vectors.

It has been found that precondensation of DNA by an additional cationic entity, prior to final encapsulation by the nanocarrier, improves its protection against degradation. Among many DNA condensing agent, protamines are the most widely used.[5,6]

Protamines are typically short proteins (50–110 amino acids) capable to condense plasmid DNA into toroid-like structures,[6,7] especially protamine sulfate. Protamine is a cell penetrating polypeptide, thanks to its richness in arginine residues containing guanidinium functional groups.[7–10] Moreover, the use of protamine in gene delivery has increased gene expression in different cell lines.[11]

The protamine/DNA weight ratio, R_W, can be adjusted, leading to either positively or negatively charged complexes. Charge modulation is a relevant property of protamine/DNA complexes, as the condensed gene payload can be coated with cationic or with anionic nanocarriers at will, thus opening the gateway to the rational design of a wide variety of gene vectors.

Although it is not doubted that the electrostatic interaction between protamine and DNA could produce compact structures,[6,12] detailed investigation of their local organization has not been reported so far. Among factors affecting protamine/DNA complexation process, DNA size is particularly relevant because it largely influences the DNA-polypeptide interaction.[13]

Several studies show that DNA fragments shorter than 3000 bp have a major transfection efficiency than longer ones. Kreiss *et al*. showed that in NIH 3T3 cells luciferase activity was about 6 times more efficient using DNA shorter than 2900 bp than it was with longer DNAs.[14] The same result was obtained in primary culture of human aortic smooth muscle (AoSMC) cells, which are much more difficult to transfect with respect to NIH 3T3 ones. In the case of AoSMC cells, the short DNA was even 77 times more efficient than the long one. The existence of an inverse correlation between DNA size and transfection efficiency has been corroborated by recent results.[15–17] Still, a well-assessed interpretation is lacking. Whatever the involved mechanism, it is now well established that all transfection barriers are strongly affected by the ultrastructural features of DNA-based complexes.[18,19]

In this study, we investigate the nanoscale structure of protamine complexes with short DNA fragments of different sizes, designed to build gene carriers in the hundreds of nanometers length-scale.

Protamine sulfate salt from Salmon (grade X) and linear Calf Thymus DNA were purchased from Sigma Aldrich and were dissolved in MilliQ filtered (0.2 μm) water at the nominal concentration of 0.1%. Such linear DNA is mimetic of plasmid-derived linearized DNAs that are often more efficient than their circular counterpart.[15]

We used ultra-tip-sonication to produce DNA fragments between 500 and 3000 bp (tipDNA). Alternatively, DNA fragments longer than 3000 bp (bathDNA) were produced by ultrasound bath sonication. Controlling the length of DNA fragments was done by gel-electrophoresis (Figure 1) on 1% agarose gel containing ethidium bromide in Tris-borate-EDTA (TBE), following a standard procedure.

Protamine/DNA complexes were prepared by dropwise addition of protamine solution to a DNA one. The overall structural properties of the complexes were obtained by light scattering and Z-potential measurements. We used a home designed apparatus, including a laser diode ($\lambda = 532$ nm), a temperature-controlled cell, and a digital correlator (Brookhaven Instruments Co.), and a ZetaPlus system (Brookhaven Instruments Co., Holtsville, NY) based on the laser

a)Author to whom correspondence should be addressed. Electronic mail: paola.brocca@unimi.it.

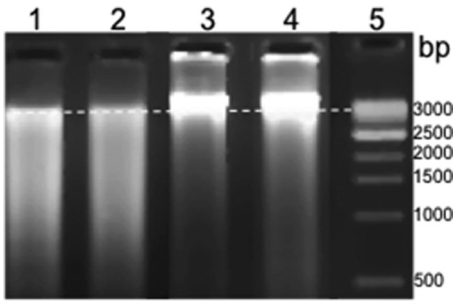

FIG. 1. DNA fragmented by ultrasonic probe-tip sonication (lanes 1 and 2) and bath sonication (lanes 3 and 4). Ladder DNA (lane 5) was used as a reference. Dashed line is a guide to the eye.

Doppler velocimetry technique. Figure 2 reports results for solutions around the charge inversion point, namely, for $R_W = 0.17, 0.25, 0.33, 0.5, 0.67$, and 1.

At low protamine content, protamine/DNA complexes are negatively charged (ZP ~ -30 mV), with hydrodynamic diameter $D_H \approx 150$ nm. For the lower protamine content, some free DNA is present in the solution, increasing its conductance. The charge inversion region occurs for $0.5 < R_W < 0.67$, where flocculation is also observed. Accordingly, electrophoresis experiments on agarose gels performed as a function of R_W show that tipDNA was completely condensed by protamine at $R_W = 0.5$ (data not shown).

At high protamine content, the system enters the re-dissolution region, characterized by the re-entrant condensation effect,[20,21] where positively charged nanoparticles (ZP > 20 mV) are formed with $D_H \approx 240$ nm.

Thus, $R_W = 0.5$ was identified as the optimum value to get maximum complexation of negatively charged nanoparticles, just before the insolubility boundary.

The local structure of protamine/DNA complexes was assessed by SAXS. Measurements were performed at the ID02 beamline at the ESRF (Grenoble, France), for different protamine/DNA R_Ws, at T = 25 °C, in the range of momentum transfer $0.017\,\text{nm}^{-1} \leq q \leq 4.65\,\text{nm}^{-1}$. Several frames were collected on each sample, 0.1 s exposure time, 1 s sleeping time, to minimize radiation damage. As first evidence, a protective effect of protamine on DNA after complexation was observed. In fact, while DNA itself suffered from radiation damage, protamine/DNA complexes were stable upon irradiation.[22]

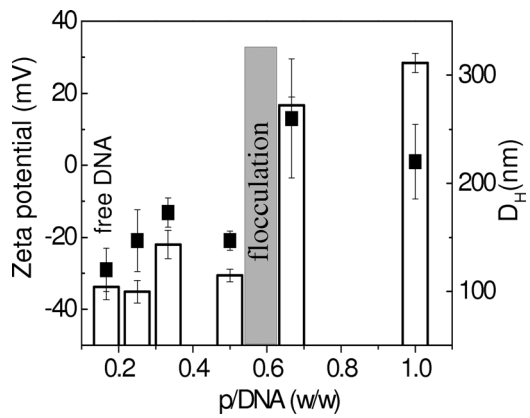

FIG. 2. Hydrodynamic diameter (squares) and Z-potential (bars) of protamine/tipDNA complexes at different R_W's.

Figure 3 reports SAXS spectra for a series of protamine/tipDNA ratios.

Two levels can be addressed: (a) a large-scale structure whose features, such as fractal dimension (power-law) and size (exponential decay), can be recognized in the low-q region of the spectra ($q < 0.1\,\text{nm}^{-1}$); and (b) a smaller substructure whose features are displayed in the high-q region of the spectra ($q > 0.1\,\text{nm}^{-1}$).

First, the low intensity of the SAXS spectrum relative to $R_W = 0.25$ (bottom spectrum in Figure 3) indicates a lower degree of complexation with respect to the others. This finding agrees with the ZP results indicating that free DNA is present in samples with low protamine content.

Second, we note that the substructure (high-q) is roughly maintained in all the spectra, while the large-scale structure seems to evolve with increasing R_W. In particular, a structure peak clearly rises, as, for protamine/tipDNA $R_W > 1$, highly positively charged interacting aggregates are present (Figure 3, inset).

SAXS data analysis has been performed, based on the unified exponential/power-law approach of Beaucage *et al.*,[23,24] suitable for polydisperse particles involving multiple levels of aggregation. The applied equation, including two structural levels is the following:

$$I(q) = \sum_{i=1}^{2} G_i \exp(-q^2 R g_i^2/3) + B_i \left\{ \left[\text{erf}(qRg_i/\sqrt{6}) \right]^3 / q \right\}^{p_i}, \quad (1)$$

where Rg_i is the radius of gyration of ith-level structure, $G_i = N_i \rho_e^2 V_i^2$ is the Guinier pre-factor and B_i is a pre-factor specific to the type of power-law scattering defined according to the regime in which the exponent p_i falls, N_i is the number density of scattering particles, ρ_e is the electron density difference between particle and solvent, and V_i is the volume of the scattering particle for each structural level.

This function includes the local exponential and power laws and the crossover from one level to the next without

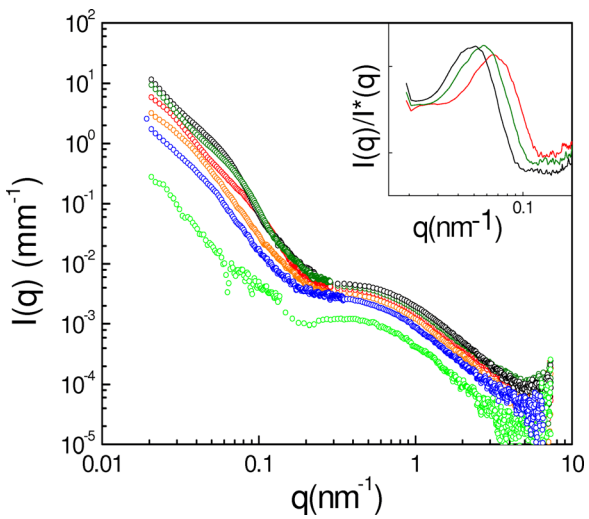

FIG. 3. SAXS spectra of protamine/tipDNA for $R_W = 3, 2, 1.5, 1, 0.5, 0.25$ (top to bottom). Inset: rising of a structure factor peak for the more charged systems, $Rw = 3$, 2, and 1.5. The corresponding I(q)s are divided by I*(q), the $Rw = 0.5$ spectrum, assumed as non interacting case.

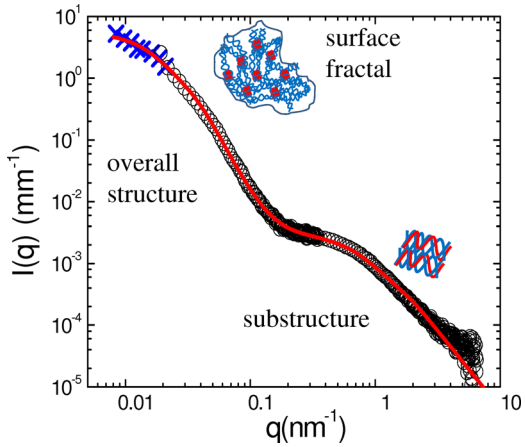

FIG. 4. SAXS intensity profile (o) of protamine/tipDNA $R_W = 0.5$ solution (c = 0.1%). Light scattering data (x) have been added in the low-q region. Solid line corresponds to the unified two levels Beaucage function reported with $G_1 = 5.76$, $Rg_1 = 101$ nm, $B_1 = 2.04 \times 10^{-6}$, $p_1 = 3.8$, $G_2 = 3.06 \times 10^{-3}$, $Rg_2 = 2.1$ nm, $B_2 = 1.44 \times 10^{-3}$, $p_2 = 2.4$.

introducing additional parameters. Therefore, the structural parameters such as the radius of gyration, polydispersity, and fractal dimension of the individual levels can be deduced in a self-consistent manner.

Fits to data are shown in Figure 4 for the experimentally more relevant sample ($R_W = 0.5$). The fitting procedure led to identify the large aggregate size (gyration radius $Rg_1 = 101$ nm) and small-scale substructures with gyration radius $Rg_2 = 2.1$ nm.

The large-scale structure is well fitted by a power-law, $p_1 = 3.8$, proper for a surface-fractal ($3 < p < 4$) with fractal dimension $d_s = 2.2$ (Ref. 23)

$$I(q) \sim q^{-(6-d_s)}. \quad (2)$$

This behaviour is consistent with globular aggregates whose surface has fractal features (power law slightly different from the Porod q^{-4} behaviour).

On the smaller scale (high-q), the substructure ($Rg_2 = 2.1$ nm) could actually correspond to the sites of protamine/DNA complexation, and can be associated to the local morphology of the complex. A high electron density (high contrast) of those sites is predictable according to a previously proposed model for Salmon-protamine complexation with DNA, consisting of two protamine molecules binding in the major groove of calf thymus DNA, with a very minor increment of the helix size.[25] The fitted $p_2 = 2.4$ power-law in the high-q region, although possibly affected by the form factor for $q > 2\,\text{nm}^{-1}$, nevertheless hints a local coil substructure rather than globular. Best-fit results suggest that the local high-contrast substructure could consist of two clamped DNA helixes bound to protamine, resembling the side-by-side protamine-mediated DNA fasciculation observed by AFM on mica substrate.[26]

Two other different model fittings were also tried: (a) one consisting of a rod-like form factor for the high-q range connected to a single-level unified function addressing the large-scale structure at lower q's and (b) the second consisting of a toroid form factor to test for a shape of protamine/DNA aggregates already found in different conditions. Neither could match the experimental SAXS profile in the intermediate q-range, and they were then discarded.

AFM from protamine/DNA complexes ($R_W = 0.5$) is reported in Figure 5.

It shows particles in the hundred-nanometers size range, quite monodisperse and with similar overall shapes. Estimation of volumes using the shapes of Figure 5, panel (b)), gives particles of equivalent radius of 80 nm, consistent with DLS and SAXS results.

In the case of longer bath-sonicated DNA fragments, protamine complexation gives rise to large aggregates that partially precipitate even in $R_W = 0.5$ proportion. Still, soluble aggregates of the appropriate size are present in the supernatant. The local structure of such complexes has been investigated by SAXS, as shown in Figure 6.

In this case, a consistent fitting can be obtained, for the high-q region, with the form factor of a long rod with cross-sectional radius of 1.1 nm, added to a single level unified function (Eq. (1) with i = 1) addressing the low-q region. The hundred-nanometers scale structure shows a power law ($p_1 = 2.7$) indicating the presence of structures of low dimensionality (mass fractal), such as percolation clusters or particles formed by non equilibrium growth processes, like diffusion limited aggregates,[27] with an estimated gyration radius $Rg_1 = 105$ nm.

Results suggest that an extended kinetically driven protamine/DNA complexation takes place, depleting clamping and preventing from optimal space-filling.

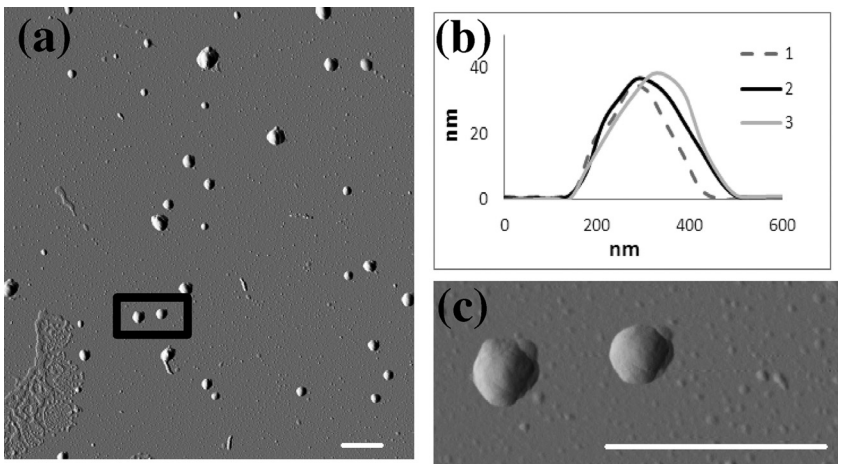

FIG. 5. Panel (a): AFM (10 μm × 10 μm) picture of a protamine/tipDNA sample ($R_W = 0.5$). The bar corresponds to 1 μm. Panel (b): Height profiles of three representative particles. Panel (c): Enlargement of a selected field of panel (a).

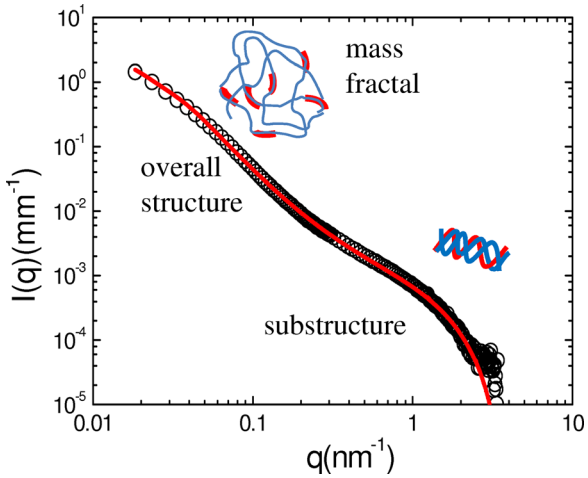

FIG. 6. SAXS intensity profile of the supernatant solution of protamine/bathDNA, $R_W = 0.5$. Solid line corresponds to the fitting function.

This concept is also supported by electrophoresis experiments on agarose gel, revealing that, when long DNA fragments are used, the complete retardation of the protamine-DNA binary complex occurs for $R_W > 1$, that is, at higher protamine-per-bp proportion as compared to short DNA fragments. The condensing ability of protamine is lower for longer DNA fragments. Moreover, it has been observed that the amount of flocculated sample strongly depends on the mixing protocol, suggesting a kinetics-dependent condensation process. This could provide a clue towards a more effective condensation of longer DNA fragments, to build small size gene vectors with enhanced ability to reach targeted cells.

To sum up, we have found that the boundary of the miscibility gap depends on the extent of DNA fragmentation, indicating that the length of DNA fragments affects the complexing ability of protamine. Whatever the extent of DNA fragmentation, the soluble complexes are in the 100 nm size range. Nonetheless, on the intraparticle scale, they show different structural properties. For smaller DNA fragments, elementary seeds of protamine-DNA complexation are found, independent on R_W. Such seeds ($Rg = 2.1$ nm) are likely to be clumping nodes for an extended DNA network. On the other hand, when protamine condenses longer DNA fragments, such small seeds are not formed, but the complex keeps the local form of a long coiled rod (1.1 nm in cross radius) that, on larger length scales, displays a less compact mass fractal structure.

Both these structures could be affected by variation in the external physico-chemical parameters like those experienced in physiological medium (pH, temperature, osmotic pressure, etc.). This issue will be addressed as a next step. In fact, both efficient DNA protection during transport, possibly connected to tight complexation with protamine, and the ability of profitable DNA release at the delivery site, maybe higher for looser substructures, are required for an effective transfection. On the other hand, playing with external parameters could be used to tune condensation while occurring, towards the best compromise between seed-type protection and ease of de-complexation, aimed to the rational design of highly efficient gene vectors.

We believe that structural studies on the pre-complexation of nucleic acid with protamine can be important also in the field of the gene silencing strategies to optimize siRNA delivery.

This work was partially supported by the Italian Minister for University and Research (MIUR) (Futuro in Ricerca, Grant No. RBFR08TLPO). Dr. C. Marchini and Dr. M. Montani are gratefully acknowledged for useful discussions and support in the electrophoresis experiments. We thank Letizia Meregalli for LS laboratory collaboration and Manuel Fernandez Martinez for technical support on ID02 beamline.

[1]G. Both, I. Alexander, S. Fletcher, T. J. Nicolson, J. E. Rasko, S. D. Wilton, and G. Symonds, Pathology **43**, 642 (2011).
[2]P. P. Denèfle, Methods Mol. Biol. **737**, 27 (2011).
[3]M. A. Kay, Nat. Rev. Genet. **12**, 316 (2011).
[4]C. J. Melief, J. J. O'Shea, and D. F. Stroncek, J. Transl. Med. **9**, 107 (2011).
[5]L. R. Brewer, M. Corzett, and R. Balhorn, Science **286**, 120 (1999).
[6]F. L. Sorgi, S. Bhattacharya, and L. Huang, Gene Ther. **4**, 961 (1997).
[7]R. Balhorn, Genome Biol. **8**, 227 (2007).
[8]S. D. Laufer and T. Restle, Curr. Pharm. Des. **14**, 3637 (2008).
[9]Y. Maitani and Y. Hattori, Expert Opin. Drug Deliv. **6**, 1065 (2009).
[10]J. B. Rothbard, T. C. Jessop, R. S. Lewis, B. A. Murray, and P. A. Wende, J. Am. Chem. Soc. **126**, 9506 (2004).
[11]H. Mima, R. Tomoshige, T. Kanamori, Y. Tabata, S. Yamamoto, S. Ito, K. Tamai, and Y. J. Kaneda, J. Gene Med. **7**, 888 (2005).
[12]N. Makita, Y. Yoshikawa, Y. Takenaka, T. Sakaue, M. Suzuki, C. Watanabe, T. Kanai, T. Kanbe, T. Imanaka, and K. Yoshikawa, J. Phys. Chem. B **115**, 4453 (2011).
[13]D. E. Olins, A. L. Olins, and P. H. Von Hippel, J. Mol. Biol. **33**, 265 (1968).
[14]P. Kreiss, B. Cameron, R. Rangara, P. Mailhe, O. Aguerre-Charriol, M. Airiau, D. Scherman, J. Crouzet, and B. Pitard, Nucleic Acids Res. **27**(19), 3792 (1999).
[15]H. Kamiya, J. Yamazaki, and H. Harashima, Gene Ther. **9**, 1500 (2002).
[16]W. Yin, P. Xiang, and Q. Li, Anal Biochem. **346**(2), 289 (2005).
[17]S. Ribeiro, J. Mairhofer, C. Madeira, M. M. Diogo, C. Lobato da Silva, G. Monteiro, R. Grabherr, and J. M. Cabral, Cell Reprogram. **4**(2), 130 (2012).
[18]G. Caracciolo and H. Amenitsch, Eur. Biophys. J. **41**, 815 (2012).
[19]G. Caracciolo, D. Pozzi, A. L. Capriotti, C. Marianecci, M. Carafa, C. Marchini, M. Montani, A. Amici, H. Amenitsch, M. A. Digman, E. Gratton, S. S. Sanchez, and A. Laganà, J. Med. Chem. **54**(12), 4160 (2011).
[20]T. T. Nguyen, I. Rouzina, and B. Shklovskii, J. Chem Phys. **112**, 2562 (2000).
[21]P.-Y. Hsiao, J. Phys. Chem. B **112**, 7347 (2008).
[22]See supplementary material at http://dx.doi.org/10.1063/1.4790588 for radiation damage protection on DNA.
[23]G. Beaucage, J. Appl. Crystallogr. **28**, 717 (1995).
[24]G. Beaucage, H. K. Kammler, and S. E. Pratsinis, J. Appl. Crystallogr. **37**, 523 (2004).
[25]V. H. Nicholas, P. M. Fred, and R. Balhorn, Biochemistry **33**, 7528 (1994).
[26]M. J. Allen, E. M. Bradbury, and R. Balhorn, Nucleic Acids Res. **25**, 2221 (1997).
[27]G. Beaucage, J. Appl. Crystallogr. **29**, 134 (1996).